International Journal of Control and Automation
Vol. 9, No. 12 (2016), pp.373-382
http//dx.doi.org/10.14257/ijca.2016.9.12.31

A Novel Research on Optimization Algorithm of Power of Solar Photovoltaic Cells

Zhenchuan Sun[1,2] and Jiasheng Zhang[1]

[1]*College of Information and Control Engineering, China University of Petroleum (East China)*
[2]*School of Mechanical and Electronic Engineering, Zaozhuang University*
szc_1983@163.com

Abstract

In order to overcome the large power fluctuation under the maximum power point of maximum power point tracking(MPPT) algorithm based on the Perturbation and Observation method(P&O) of traditional solar photovoltaic(SPV), an optimization algorithm based on the three-order difference of power and variable step is presented. In the traditional P&O of MPPT of SPV, the first-order difference of the power is elected as the variation of the power. When the SPV is operated nearby the voltage of maximum power point, the traditional algorithm has its limitation that the power will present the approximate equal amplitude oscillation under the maximum power point because of the false judgment of the algorithm. By analyzing the relationship between the three-order difference of the power and the relative position of the operating point and the maximum power point, the next variation trend of the operating point is presented. The variable step algorithm is applied so the SPV will operate again according to the algorithm based on the three-order difference of power and variable step when the operating point cross the maximum power point first. The correctness and rationality of the proposed algorithm is tested by the results of the Matlab/Simulink.

Keywords: *Solar Photovoltaic cells; Perturbation and Observation method; three-order difference of power; maximum power point tracking; variable step*

1. Introduction

Energy is the foundation of survival and development of human. As the most clean and convenient form of energy, electricity plays an important role in national economic development. Because of its high power line transmission loss and operating costs as well as instability caused by sudden natural disasters, conventional large power grid as the main power supply channel can accelerate the theoretical and technical research on distributed generations and other related fields objectively which will not only promote utilization efficiency of traditional energy, but make full use of various renewable energy. With the development of power electronic conversion technique and control theory, as a combination of distributed generation, load, energy storage devices and control devices, micro grids have multifunction such as power generation, heating and other services with obvious advantages in effective improvement of cascade utilization of energy and reliability of system. As a form of distributed energy, SPV technology has developed rapidly in recent years. SPV cells are characterized by simple structure, small size, clean and free of noise, high reliability, long service life and so on. For making full use of solar energy, maximum power output should be ensured based on volt-ampere characteristics of SPV arrays when they are operated [1].

Numerous studies on MPPT control algorithm of SPV have been carried out by domestic and foreign scholars. Perturbation and observation method and conductance increment method are two most basic control algorithms, but both methods could bring

ISSN: 2005-4297 IJCA

power fluctuation caused by misjudgment when the system is operated nearby the voltage of maximum power point, so that it is difficult to accurately control the output power of the system[2].Short-circuit current method[3][4] requires a switch to determine the short-circuit current, while open circuit voltage method[5][6] needs to temporarily disconnect the DC-DC converter for periodic measurements of open circuit voltage, both of which could bring power loss. SMVSC [7][8] can accurately track the maximum power point, but hardware implementation is more complex. Fuzzy neural algorithm[9][10] combines fuzzy control algorithm and neural network control algorithm the optimum voltage corresponding to maximum power point is regulated by neural network controller, while duty ratio of the DC-DC converter is regulated by fuzzy controller. In addition, linear control strategy based on state space has been applied in MPPT control of SPV[11].

Based on the power-voltage (P-V) curve analysis of SPV cells, limitations of the P&O based on the first-order difference was summarized and control algorithm based on the third-order difference with variable steps was proposed. The relationship between third-order difference and relative position of system operating point and maximum power point was analyzed, by modifying the traditional perturbation and observation method, the oscillation amplitude of output power nearby the maximum power point was reduced remarkably. Application of variable-step algorithm can make the system operating point run once again based on the proposed algorithm after the maximum power point was operated for the first time. The correctness and rationality of the proposed algorithm was tested by the simulation results.

2. Principle of Traditional P&O

2.1. P-V curve of SPV Cells

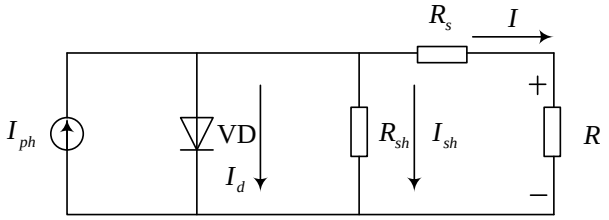

Figure 1. The Equivalent Circuit of Solar Photovoltaic

The equivalent circuit of SPV cells is shown in Figure 1. Its volt-ampere characteristics can be expressed by the formula below [12]:

$$I = I_{ph} - I_0 \left\{ \exp\left[\frac{q(U + IR_s)}{AKT} \right] - 1 \right\} - \frac{U + IR_s}{R_{sh}} \quad (1)$$

Where, I is the load current; I_0 is the reverse saturation current; q is the electronic charge (1.6×10^{-19}C); U is the terminal voltage of the load; A is ideality factor of PN junction; K is Boltzmann's constant (1.38×10^{-23}J/K); T is the absolute temperature; R_s is the series resistance of SPV cells; R_{sh} is the parallel resistance of SP cells.

Then, P-V curve of SPV cells under the conditions that the light intensity S is equal to 1000 W/m^2 while the temperature $T = 50$°C (323K) can be obtained, as shown in Figure 2.The maximum output power of SPV cells P is equal to 1243W when the terminal voltage of SPV is equal to 50.3V.

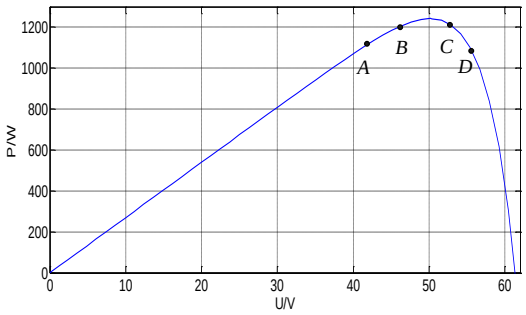

Figure 2. The Power-Voltage Curve of Solar Photovoltaic

2.3. Analysis of Limitations of Traditional P&O

In the traditional P&O, a small increment is periodically applied to the output voltage of photovoltaic array, and the change trend of the output power is observed. If the output power increases with the increase of voltage, voltage should increase more. If the output power decreases on the same condition, voltage should be decreased reversely. If the output power increases with the decrease of voltage, voltage should be decreased continuously. If the output power decreases on the same condition, voltage should be increased reversely. However, this method could bring misjudgment when the system operating point is close to the maximum power point. Analysis is conducted as follows:

As shown in Figure 2, when the system operating point is located at point C, with previous operating point being assumed to be A, then the power increases with the increase of voltage from point A to point C; therefore, the voltage should be increased more according to the analysis above. However, the voltage has transcended the voltage corresponding to maximum power point at this time, then continuous increase of voltage will make the power output of SPV cells deviate from the maximum power point, and the oscillation amplitude nearby the maximum power point will become large. Similarly, when the system operating point is located at point B, while previous operating point is assumed to be D, then the power increases with the decrease of voltage from point D to point B; therefore, the voltage should be continued to decrease. However, the voltage has been over the voltage corresponding to maximum power point at this time, then continuous decrease of voltage will make the power output of SP cells deviate from the maximum power point, and the oscillation amplitude nearby the maximum power point will become large.

3. Principle of Third-order Power Difference

As can be seen from the analysis of limitations of traditional P&O, it is the key that the position of current system operating point with respect to the maximum power point as well as symbol of differences between the current voltage with respect to one of sampling time can be properly judged which may provide fast convergence of the system operating point to maximum power point as well as reduction of oscillation amplitude. In the traditional P&O, the first-order differences of power provide the SPV system with more misjudgment nearby the maximum power point, as well as larger oscillation amplitude and oscillation frequency of power.

Suppose that the output power P of SPV cells is regarded as the function of the output voltage V , it is a function of one variable that is $P = f(V)$ .The function curve is assumed to be smooth enough, and the voltage corresponding to the maximum power point is assumed to be V_m , so all-order derivatives of the function $P = f(V)$ exist at

point V_m and its neighborhood domain.

Based on the P-V curve of SPV cells , the power increases with the increases of the voltage with its left neighbourhood domain $(V_m-\delta,V_m)$,so $\frac{dP}{dV}>0$,while the power decreases with the increases of the voltage with its right neighbourhood domain $(V_m,V_m+\delta)$,and $\frac{dP}{dV}<0$.

According to the analysis above, $\frac{d^2P}{dV^2}<0$ on the condition that V lies in its neighbourhood domain $U(V_m,\delta)$.The fact that $\frac{dP}{dV}$ is a monotone decreasing function can be derived including equations $\left.\frac{dP}{dV}\right|_{V=V_m}$ =0 and $\left.\frac{d^2P}{dV^2}\right|_{V=V_m}$ =0.

In the maximum power control system of SPV, the discrete control system has been applied to realize judgment and tracking of the power and the voltage. Therefore, the In order to analyze the characteristics of output power of SPV cells in the vicinity of the maximum power point and calculate the third-order difference, partial P-V curve graph of SP cells is enlarged, as shown in Figure 3.

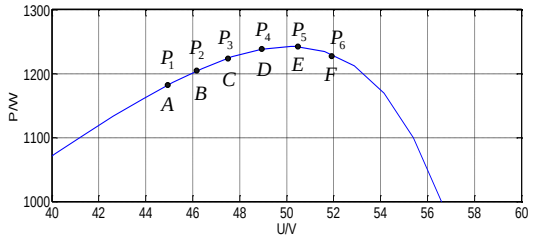

Figure 3. The Partial Power-Voltage Curve of Solar Photovoltaic

In Figure 3, the voltage range is 40V ~ 60V, and the power range is 1000W ~ 1243W. Points $A\sim F$ indicate the system operating points corresponding to six consecutive sampling intervals, respectively, while $P_1\sim P_6$ indicate the output power, of which point E indicates that SPV cells are working at the maximum power point with the maximum power $P_5=1243\text{W}$.

The third-order difference of output power of SPV cells can be expressed as:

$$\begin{aligned}&\nabla^3P(k)=\nabla(\nabla^2P(k))=\nabla^2P(k)-\nabla^2P(k-1)=\nabla(\nabla P(k))-\nabla(\nabla P(k-1))\\&=\nabla(P(k)-P(k-1))-[\nabla(P(k-1)-P(k-2))]=\{[P(k)-P(k-1)]\\&-[P(k-1)-P(k-2)]\}-\{[P(k-1)-P(k-2)]-[P(k-2)-P(k-3)]\}\\&=P(k)-3P(k-1)+3P(k-2)-P(k-3)\end{aligned}\tag{2}$$

Therefore, at point *D*,

$$\nabla^3P_D=[(P_4-P_3)-(P_3-P_2)]-[(P_3-P_2)-(P_2-P_1)]=P_4-3P_3+3P_2-P_1\tag{3}$$

$$\begin{aligned}&\nabla^3P_F=[(P_6-P_5)-(P_5-P_4)]-[(P_5-P_4)-(P_4-P_3)]\\&=[-(P_5-P_6)-(P_5-P_4)]-[(P_5-P_4)-(P_4-P_3)]\\&=P_6-3P_5+3P_4-P_3\end{aligned}\tag{4}$$

The first-order derivatives of the system power at various points of $A \sim F$ to voltage are assumed to be $k_1 \sim k_2$, respectively, and the system sampling time is assumed to be ΔT, then

$$k_1 = \left.\frac{dP}{dV}\right|_A, k_2 = \left.\frac{dP}{dV}\right|_B, k_3 = \left.\frac{dP}{dV}\right|_C, k_4 = \left.\frac{dP}{dV}\right|_D, k_5 = \left.\frac{dP}{dV}\right|_E, k_6 = \left.\frac{dP}{dV}\right|_F$$

$$k_1 > k_2 > k_3 > k_4 > k_5 = 0 > k_6, \tag{5}$$

Assume

$$k_3 > -k_6 > k_4 \tag{6}$$

Based on the calculus,

$$P_6 - P_5 = -(P_5 - P_6) \approx -k_6 \Delta T, P_5 - P_4 \approx k_4 \Delta T, P_4 - P_3 \approx k_3 \Delta T,$$
$$P_3 - P_2 \approx k_2 \Delta T, P_2 - P_1 \approx k_1 \Delta T, \tag{7}$$

We can obtain following results,

$$\nabla^3 P_D \approx [k_3 - k_2 - (k_2 - k_1)]\Delta T = (\frac{k_3 - k_2}{\Delta T} - \frac{k_2 - k_1}{\Delta T})(\Delta T)^2$$
$$\approx (\left.\frac{d^2 P}{dV^2}\right|_B - \left.\frac{d^2 P}{dV^2}\right|_A)(\Delta T)^2 \tag{8}$$

$$\nabla^3 P_F \approx [-k_6 - k_4 - (k_4 - k_3)]\Delta T = \{-[k_4 - (-k_6)] - (k_4 - k_3)\}\Delta T \tag{9}$$

Within the neighborhood domain $U(V_m, \delta)$, since $\frac{d^2 P}{dV^2} < 0$, then, $\nabla^3 P_D < 0, \nabla^3 P_F > 0$. Therefore, when the operating point is located nearby the maximum power point, its position with respect to the maximum power point can be obtained through calculating the third-order difference of the power at operating point. Then, change trend of voltage in the next sampling time can be controlled properly based on the P&O method, so as to quickly approach the maximum power point and reduce oscillation amplitude at the same time.

4. Principle of Variable Step Algorithm

When the system operating point exceeds the maximum power point for the first time, for the reason that the system operating point is located within the right neighbourhood domain $(V_m, V_m + \delta)$ of the output voltage, therefore, sign of the third-order difference of the power will change reversely. If the control step is changed by the law of geometric progression at this time, the output voltage will be controlled according to the algorithm above once the operating point exceeds the maximum power point.

Assume that the original step is l, and the next step with the operating point exceeding the maximum power point is l_1, then

$$l_1 = ql, q < 1, \tag{10}$$

At this moment, the system operating point will reversely exceed the maximum power point. Assume that the number of the exceedings of the system operating point is n, which is an even number including two $n/2$ of both positive number and negative number. So the step after exceeding the maximum power point for the n-th time is:

$$l_n = q^n l, q < 1 \tag{11}$$

Since the step will be decreased based on geometric progression once the maximum power point was exceeded, therefore, the output voltage and the output power of each reverse exceeding can be controlled in accordance with the above-mentioned algorithm

based on the third-order power difference. After the first forward exceeding, the symbol of the third-order difference of the power is opposite to the previous one.

Suppose that M_i and N_i ($i = 2, \cdots, n$) show the operating point when the system crosses the maximum power point for the i-th time which is near to the maximum power point, respectively, then

$$P_{M_i} < P_{\max} < P_{N_i}$$

So, when $i = 1, 3, 5, \cdots, 2k+1$, the moving trend of the system operating point which exceeds the maximum power point is from point M_i to point N_i. The conclusion $\nabla^3 M_i > 0$ and $\nabla^3 N_i < 0$ can be easily derived. As the special example, point M_1 and point N_1 express the point D and point F which are mentioned above.

In case of $i = 2, 4, \cdots, 2k$, the movement trend of the system operating point is from point N_i to point M_i reversely with the conclusion including $\nabla^3 M_i > 0$ and $\nabla^3 N_i < 0$.

Therefore, after the step is changed each time, change trend of voltage can be controlled correctly according to the symbol of the third-order power difference of the system operating point nearby the maximum power point, and the system can be converged to the maximum power point and the oscillation amplitude can be reduced remarkably.

5. Simulation Results and Analysis

The simulation based on the improved optimization control algorithm of three-order difference and variable steps is presented by Matlab/Simulink as follows. The control system block diagram is shown in Figure 4:

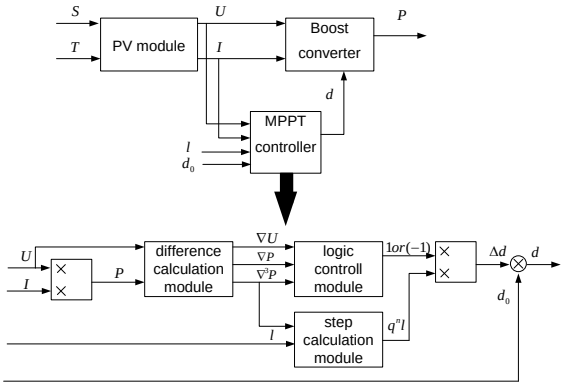

Figure 4. The Control System Block Diagram of MPPT of Solar Photovoltaic

The parameters used for simulation are as follows: in case of the ambient temperature $T = 25\,°\text{C}$, the open circuit voltage of SPV cells $V_{OC} = 61.25\,\text{V}$, the short-circuit current $I_{SC} = 27.03\,\text{A}$, the voltage corresponding to the maximum power point $V_{mp} = 50.3$ V, the current $I_{mp} = 24.7$ A, current temperature coefficient of SPV cells $\alpha = 0.0025$ A/°C(K), voltage temperature coefficient $\beta = 0.00288$ A/°C(K). The simulation results are shown in Figure 5 ~ 7:

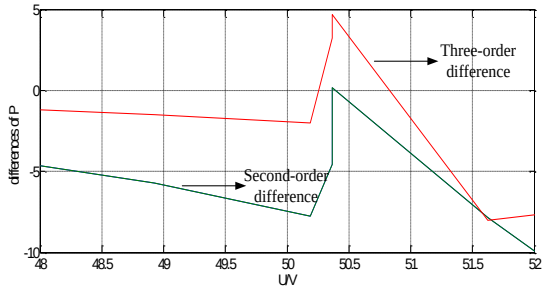

Figure 5. Partial Enlarged Views of the Second-Order Difference and Third-Order Difference of Output Power of Solar Photovoltaic

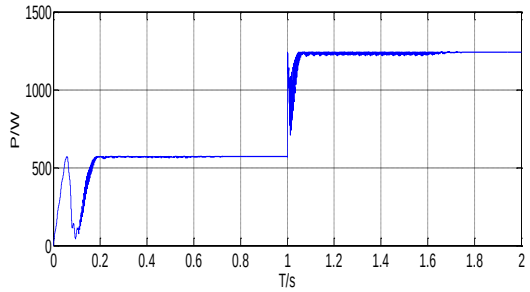

(a)

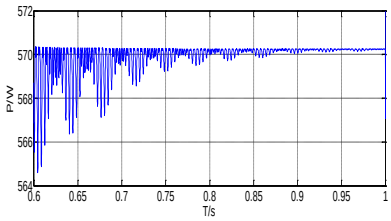

(b)

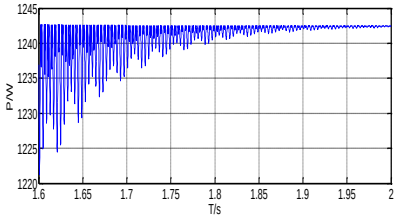

(c)

Figure 6. Output Power of Solar Photovoltaic and Partial Enlarged Views

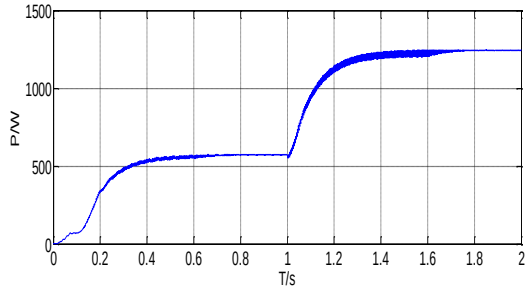

(a)

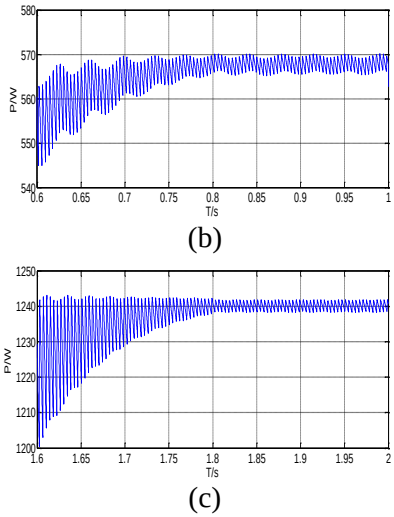

Figure 7. Output Power of Boost Converter and Partial Enlarged Views

Figure 5 shows the partial enlarged views of the second-order difference and third-order difference of output power of SPV cells. As can be seen from the Figure 5, in case of the output voltage of SPV cells from 48V to 52V, the second-order difference of the power is negative, and in case of the output voltage $V = V_{mp} = 50.3$ V, the second-order difference of the power is zero. In case of the output voltage of SPV cells changes from 50.2V to 50.4V, the third-order difference of the power monotonically increases, and in case of the output voltage $V = V_{mp} = 50.3$ V, the third-order difference of the power is zero. Therefore, in the vicinity of the maximum power point of SPV cells, the third-order difference of the power can be used as the basis for determining the relative position of output voltage operating point and maximum power point as well as the next movement trend.

Figure 6 shows the output power of SPV cells and its partial enlarged views. Within 0 ~ 1s, the ambient parameters of SPV cells are: $S = 500$ W/m2, $T = 20$ ℃; within 1 ~ 2s, the ambient parameters of SPV cells are: $S = 1000$ W/m2, $T = 50$ ℃. As can be seen from Figure 6 (a), the output power of SPV cells is stabilized at 571W after 0.2s. To compare with the traditional P&O algorithm, the traditional P&O algorithm is used before 0.6s, and the improved P&O algorithm proposed in this paper is operated after 0.6s; after the ambient parameters are changed, the traditional control algorithm is used before 1.6s, while the improved one proposed in this paper is operated after 1.6s. Figure 6 (b) and (c) are the partial enlarged views of Figure 6 (a) after the improved control algorithm is used, respectively. As can be seen from Figure 6 (b), output power of SPV cells is within 564W and 571W before 0.6s, as the approximate persistent oscillation process; after 0.6s, the output power of SPV cells gradually approach the maximum power because of the application of improved algorithm proposed in this paper. After 0.8s, the error of the output power and the maximum power is less than 1W. As can be seen from Figure 6 (c), the output power of SPV cells is within 1220W and 1243W before 1.6s, as the approximate persistent oscillation process, too. After 1.6s, the output power of SPV cells gradually approach the maximum power, after 1.8s, the error of the output power and the maximum power is less than 2W.

Figure 7 shows the output power of Boost converter and its partial enlarged views. The ambient parameters and control algorithms are consistent with those of Figure 6. Figure 7 (b) and (c) are the partial enlarged views of Figure 7 (a) after the improved control algorithm is used, respectively. The trend of output power of the boost converter is consistent with the trend of the output power of SPV cells. As can be seen from Figure 7

(b), the output power of SPV cells is within 564W and 570W before 0.6s, as the approximate persistent oscillation process. After 0.6s, the output power of SPV cells gradually approach the maximum power after 0.8s, the error of the output power and the maximum power is less than 1W. As can be seen from Figure 7 (c), the output power of SPV cells is between 1220W and 1243W before 1.6s, as the approximate persistent oscillation process. After 1.6s, the output power of SPV cells gradually approach the maximum power, while, after 1.8s, the error of the output power and the maximum power is less than 2W.

The correctness and rationality of maximum power point tracking optimization algorithm based on the third-order difference and variable steps of SPV cells has been verified by the simulation results and analysis of Figures 5 ~ 7.

Acknowledgements

First of all, I would like to extend my sincere gratitude to my supervisor, Zhang Jiasheng, for his instructive advice and useful suggestions on my thesis. I am deeply grateful of his help in the completion of this thesis. I am also deeply indebted to all the other tutors and teachers for their direct and indirect help to me. Finally, I am indebted to my mother and my wife for their continuous support and encouragement.

References

[1] J. Zhang and W. Huang, "Operation control and protection technology of Microgrid", China Electric Power Press,Beijing, **(2009)**.
[2] G. Dileep and S.N. Singh, "Maximum power point tracking of solar photovoltaic system using modified perturbation and Observation method", Renewable and Sustainable Energy Reviews, vol. 50, **(2015)**.
[3] K. Kobayashi, I. Takano and Y. Sawada, "A study on a two stage maximum power point tracking control of a photovoltaic system under partially shaded insolation conditions", Proceedings of the IEEE Power Engineering Society general meeting, Toronto, Canada, **(2003)**.
[4] P. Jun, W. Chenghua and H. Feng, "Research of photovoltaic charging system with maximum power point tracking", Proceedings of the ninth international conference on electronic measurement &instruments ICEMI'2009, Beijing, China, **(2009)**.
[5] C.W. Jung, J.H. Liahng and W.J. Chang, "Maximum power point tracking method for the voltage-mode grid-connected inverter of photovoltaic generation system", International Conference on Sustainable Energy Technologies (ICSET), Singapore, Singapore, **(2008)**.
[6] M. Sokolov and D. Shmilovitz, "Photovoltaic maximum power point tracking based on an adjustable matched virtual load", APEC 07-Twenty-Second Annual IEEE Applied Power Electronics Conference and Exposition, California, America, **(2007)**.
[7] K. Il-Song, M.-B. Kim and M.-J. Youn, "New maximum power point tracker using sliding-mode observer for estimation of solar array current in the grid-connected photovoltaic system", IEEE Transactions on Industrial Electronics, vol.53, no.4, **(2006)**, pp. 1027-1035.
[8] R. Aghatehrani and R. Kavasseri, "Sensitivity-analysis-based sliding mode control for voltage regulation in microgrids", IEEE Transactions on Sustainable Energy, vol.4, no.1, **(2006)**, pp. 50-57
[9] H.H. Lee, L.D. Khoa, L.M. Phuong and P.Q. Dzung, "The New Maximum Power Point Tracking Algorithm using ANN-Based Solar PV Systems", TENCON 2010-2010 IEEE Region 10 Conference, Fukuoka, Japan, **(2010)**.
[10] M.A. Younis, T. Khatib, M. Najeeb and A.M. Ariffin, "An improved maximum power point tracking controller for PV systems using artificial neural network", Przegląd Elektrotechniczny (Electrical Review), **(2012)**.
[11] S.V. Eugene, L. Shengyi and A.D. Roger, "Power controller design for maximum power point tracking in solar installations", IEEE Transactions on Power Electronics, vol.19, no.5, **(2004)**, pp. 1295-1304.
[12] C. Wang, "Analysis and Simulation Theory of Microgrids.Science Press", Beijing, **(2013)**.

Authors

Zhenchuan Sun, he was born in Shandong province of China in 1983.He received the B.S. and M.S. degrees from Shandong University in 2005 and 2008 respectively. Since 2009, he has been a lecturer of Zaozhuang University. He has been a Ph.D candidate of College of Information and Control Engineering of China University of Petroleum (East China) since 2014. His research interests include control theory and application, distributed generation and DC microgrids.

JiaSheng Zhang, he was born in Shandong, China in 1957. He received his B.S. degree in applied electronic technology from China University of Petroleum, Shandong, China in 1982 and M.S. and Ph.D. degrees in electrical and electronic engineering from Beijing Jiaotong University, Beijing, China in 1988 and 1998, respectively. In 1982, he joined the Department of Electrical Engineering at China University of Petroleum, Shandong, China, where he is currently employed full time as a professor. His current research interests include power electronics, motor drives, power quality control, renewable distributed power sources, and DSP-based control of power converters.